Hartree–Fock Minimal and Extended Basis Set and Configuration Interaction Calculations on the Hydroboration Reaction

Kenneth R. Sundberg,[1] Glenn D. Graham, and William N. Lipscomb*

Contribution from the Department of Chemistry, Gibbs Laboratory, Harvard University, Cambridge, Massachusetts 02138. *Received November 20, 1978*

Abstract: The hydroboration reaction is studied at several levels of approximation. The partial retention of diatomic differential overlap (PRDDO) method is used to determine the molecular structures of the reactants and products and a metastable intermediate involved in the reaction. Alternative reaction paths connecting these structures are determined with the linear synchronous transit and orthogonal optimization methods, and the reaction is found to pass through the metastable geometry. Extended basis set calculations are performed for several points along the reaction path, and, even though the reaction and activation energies are different from the PRDDO results, the two potential curves show some qualitative similarity, and the reaction transition state is predicted to have nearly the same path coordinate in both sets of calculations. The electronic structure of the transition state is interpreted by a population analysis of the extended basis wave function, and these data combined with an unusual orbital correlation diagram show the reaction to proceed through a two-step donation-back-donation mechanism. Configuration interaction calculations on the closed-shell wave functions for various species in the reaction system show that correlation energy stabilizes the transition state relative to the reactants and the products; in fact, at the zero-order configuration interaction level, the reaction has no activation barrier.

Introduction

The hydroboration reaction is an interesting and important process in organic synthesis.[2-4] The basic reaction is the reversible addition of a borane to an unsaturated hydrocarbon to yield an organoborane that can be altered to form a variety of new substances. Usually anti-Markownikoff addition of hydrogen results,[5] but the addition may be Markownikoff depending on any of several directive effects. Such effects originate in steric factors created by various substitutions to the borane or to the hydrocarbon;[6-10] or, more interestingly, they may be created by the presence of electron-donating or electron-withdrawing groups substituted to the hydrocarbon.[11-14] Naturally, a full understanding of these effects depends on a knowledge of the molecular and electronic structure of the transition state for the hydroboration reaction.

The stereochemistry of the hydroboration reaction suggests that it goes through a four-center transition state.[11,13,15] For the hydroboration of an olefin, this view would have the boron atom of a borane molecule attack one carbon of an unsaturated site while one of the hydrogen atoms of the borane molecule attacks the other. One naturally conjectures that such a process involves a transition state in which the olefin π bond and one of the boron–hydrogen bonds in the borane are weakened while the carbon–boron and carbon–hydrogen bonds in the organoboranes are being formed.

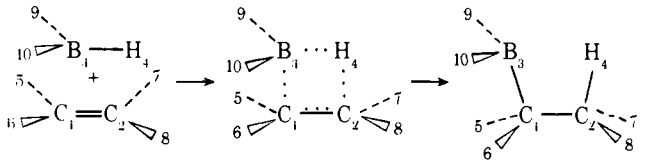

The formation of the transition state and its distortion to the final reaction products is thought to be facilitated by the vacant orbital on the boron atom, B_3. The transition state above is usually characterized as a donation–back-donation structure. The olefin is thought to donate electrons to the borane, primarily through carbon C_1, to the vacant orbital on B_3, at the same time as the borane hydrogen, H_4, donates electrons back to the olefin, primarily at C_2. This charge redistribution weakens the C_1C_2 π bond and the B_3H_4 σ bond while partially forming C_1B_3 and C_2H_4 bonds; continuation of the motion finally produces the organoborane.

In another view, the hydroboration reaction proceeds through an intermediate π complex held together by a three-center bond.[15] The complex forms because of attractive forces between the olefin π cloud and the vacant orbital of the borane, and the organoborane forms through a continuous distortion of the orbitals in the intermediate over into the orbitals of the final reaction product. The three-center $C_1B_3C_2$ bond of the

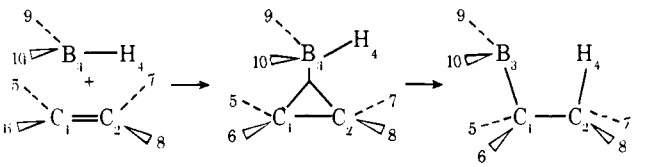

intermediate goes over into the C_1B_3 bond of the organoborane, and the B_3H_4 bond of the intermediate goes over into the C_2H_4 bond of the final product. Arguments against this intermediate are raised on stereochemical grounds,[16] but most of these objections can be met in one way or another.[17]

The donation–back-donation mechanism is a description of a transition state, but the π-complex mechanism as commonly advanced is the description of an intermediate. Since an intermediate is at an energy minimum, it must pass over a transition-state barrier to complete the reaction. We must allow for the possibility that this transition state, encountered on the last leg of the π-complex mechanism, is formally the same as the transition state encountered in the donation–back-donation mechanism.[12] Further, a careful analysis of the molecular and electronic structure of the transition state is required before it can really be classified as either a π complex or a donation–back-donation structure. These mechanistic problems as well as the determination of the system's reaction and activation energies can be addressed by a careful theoretical analysis of the problem.

This paper presents a molecular orbital (MO) study of the addition of a borane to an olefin using borane and ethylene as a model system. The reaction paths we considered are shown in Scheme I. We call the path from III to IV to V path 1, corresponding to the π-complex scheme discussed above; we call the path from III to IV′ to V path 2, corresponding to the donation–back-donation mechanism above; and finally, we call the path from III to IV to IV′ to V path 3, corresponding to the existence of a loosely bound π complex which must go through

Table I. PRDDO Calculated Molecular Structures[a] of Intermediate Conformations in the Hydroboration Reaction

structure	I	II	III		IV			V	VI
P			1.0	0.669	0.585	0.497	0.340	0.0	
$R(C_1C_2)$		2.5183	2.5363	2.5844	2.5967	2.6898	2.9283	2.9360	2.9198
$R(C_1B_3)$			5.6255	4.0923	3.7147	3.3122	2.9667	3.0243	3.0037
$R(C_2H_4)$			5.9468	4.5047	4.1343	3.4853	2.3190	2.0740	2.0753
$R(B_3H_4)$	2.2738		2.2615	2.2561	2.2595	2.3730	2.9741	4.7583	6.6464
$R(C_1H_5)$		2.0694	2.0731	2.0753	2.0758	2.0720	2.0733	2.0694	2.0727
$R(C_2H_7)$		2.0694	2.0731	2.0776	2.0787	2.0916	2.0761	2.0746	2.0723
$R(B_3H_9)$	2.2738		2.2665	2.2465	2.2415	2.2459	2.2439	2.2714	2.2741
$\measuredangle C_2C_1B_3$			77.45	71.89	70.02	71.80	75.67	107.83	108.49
$\measuredangle C_1C_2H_4$			98.85	101.30	124.11	114.67	107.69	112.62	110.78
$\measuredangle C_2C_1H_5$		122.61	121.14	121.59	121.65	119.32	116.13	110.15	104.34
$\measuredangle B_3C_1H_5$			97.79	105.34	107.26	112.54	118.07	111.23	111.30
$\measuredangle C_1C_2H_7$		122.61	121.42	121.49	121.48	120.62	114.52	111.70	111.96
$\measuredangle H_4C_2H_7$			87.15	90.26	90.31	93.91	102.63	106.57	107.14
$\measuredangle H_9B_3H_{10}$	120.00		121.94	119.72	117.70	119.69	123.50	117.98	117.81
$\measuredangle C_1B_3H_9$			80.9	94.20	97.43	106.64	117.74	120.99	121.08
E	−26.340 94	−77.876 60	−104.223 86	−104.243 73	−104.248 46	−104.245 86	−104.288 70	−104.325 62	−104.330 25
$-E/T$	1.007	1.005	1.006		1.007	1.007		1.006	1.006

[a] Bond lengths and energies in au, angles in degrees.

Scheme I

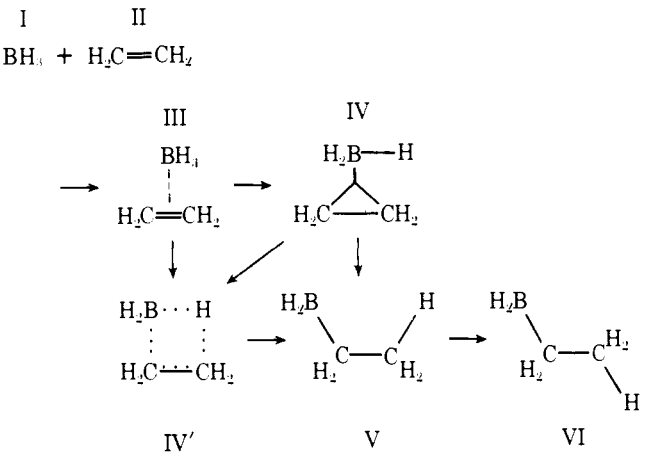

a polarized transition state of the type we would expect for path 2. The details of the formation of III from I and II and of the rotational inversion of V to VI are not discussed here. However, species I, II, and VI are essential to the evaluation of the system's reaction and activation energies, so their structures must be determined.

The structures of the molecules and transition states involved in these paths are calculated using the partial retention of diatomic differential overlap (PRDDO) approximation[18,19] to the Hartree–Fock self-consistent field (SCF) theory. The reaction paths are found using the linear synchronous transit (LST)[20,21] method and the related technique of orthogonal optimization.[20,21] The potential surfaces are then recalculated using an extended Gaussian basis set (4-31G)[22] and the SCF theory. Analyses of these latter wave functions are used to characterize the charge redistribution and bonding changes that occur during the reaction. Finally, the correlation energy contributions to the reaction and activation energies are estimated using a zero-order configuration interaction (CI) wave function based on an SCF closed-shell wave function composed of MOs expanded in an extended Slater-type orbital (STO) basis set.

Molecular Structures

The structures of I–IV are calculated by optimizing the energy produced by a PRDDO wave function. We assume that each system has at least the symmetry of point group C_s, and for structures I, II, IV, V, and VI every parameter defining a model geometry is sequentially optimized several times to assure that a minimum is really produced. Structure III is chosen just to allow a comparison of different reaction paths for the formation of V, and so its structure in somewhat arbitrary. We obtain III from IV by translating the BH_3 unit 2.0 au away from the $H_2C{=}CH_2$ unit along a line from the B atom to the center of the CC bond; all of the other parameters are then optimized as discussed above. The final geometries and energies may be found in the appropriately labeled columns of Table I. All of the optimizations used Slater exponents in the minimal basis set of the PRDDO method, and all of the structures except III correspond to stationary points on the PRDDO energy surface.

The final PRDDO reaction energies for the production of IV and VI from I and II are −19 and −71 kcal/mol, respectively. These values are very exothermic with respect to the corresponding experimental reaction energy[23] of −33 kcal/mol and to other theoretical work. Several effects could cause this discrepancy. For one, both I and II are molecules used in the original PRDDO parametrization, so the method probably describes these two systems rather better than it does some other molecules like IV and V. Since PRDDO always tends to underestimate the total energy relative to an ab initio minimum basis set calculation, we expect it to overstabilize IV and V with respect to I and II. Alternatively, the problem could be a defect in the minimal basis set method itself that makes it inadequate to describe the hydroboration reaction. To resolve this question, one must compare the PRDDO calculations to a calculation that really does reproduce the true minimal basis set results. To do so, the PRDDO method was employed with Pople exponents,[24,25] and the geometries of I, II, IV, and V were redetermined. STO-6G[25,26] calculations were performed at these geometries, and the energies produced by the two methods[27] are shown in Table II. Both PRDDO and STO-6G underestimate the energies of IV and V relative to I and II. Therefore, the errors in the PRDDO prediction of the reaction and activation energies should be ascribed to errors in the minimal basis set method or to correlation effects.

The geometries predicted by PRDDO for I, II, IV, and V are very reasonable, however. The geometry of II is consistent with experiment,[28] and the geometry of I is consistent with other theory.[29] The geometries of V and VI correspond well to other theoretical work[30] and with standard model values.[30,31]

Table II. Comparison of PRDDO and STO-6G Calculations of the Total Energy[a] of Several Molecules[b] in the Hydroboration Reaction

wave function	I	II	IV	Δ_{IV}[c]	V	Δ_V[c]
PRDDO	−26.3572	−77.8962	−104.2820	−0.0286	−104.3641	−0.1107
STO-6G	−26.3311	−77.8282	−104.1682	−0.0089	−104.2510	−0.0917

[a] Energy in au. [b] Geometries determined by PRDDO with Pople exponents (ref 24 and 25). [c] Energy relative to the sum of I and II.

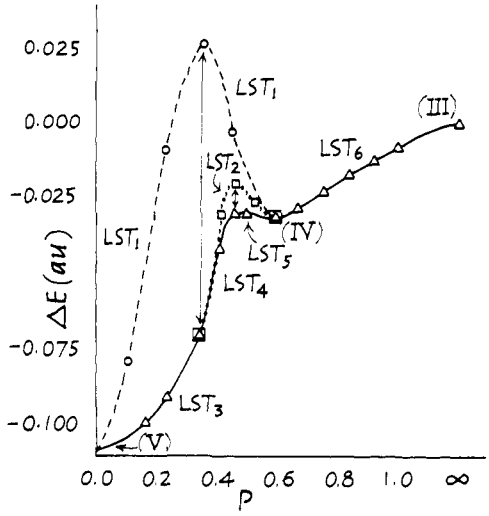

Figure 1. Linear synchronous transit pathways for the reaction of a borane ethylene complex (III) to form ethylborane (V) via the intermediate IV.

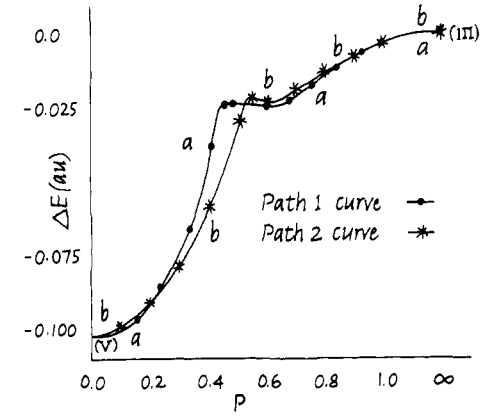

Figure 2. PRDDO potential curves for the reaction of a borane ethylene complex (III) to form ethylborane (V) via the intermediate IV, path 1, and via a direct route, path 2.

Table III. Comparison of the Molecular Structures[a] of the Transition States Defined by Paths 1 and 2

path	$R(C_1C_2)$	$R(C_1B_3)$	$R(C_2B_3)$	$R(C_2H_4)$	$R(B_3H_4)$
1	2.69	3.31	3.56	3.49	2.37
2	2.69	3.30	3.51	3.36	2.45

[a] Bond lengths in au.

Given these facts, we tentatively accept PRDDO as a structural theory for this system, but we need to look elsewhere for good predictions of the reaction and activation energies.

Reaction Pathways and Transition States

Path 1 consists of two segments connecting three well-defined structures: III, IV, and V. To determine this path the linear synchronous transit (LST) method and orthogonal optimizations are used to find a sequence of molecular transformations that carry III to IV and IV to V. To begin, structures III and V are given path coordinate[20] values $P = 1.0$ and 0.0, respectively. The path coordinate of IV is determined with respect to III and V, and it is given by $P = 0.585$. Since path 1 consists of two independent segments, they are determined one at a time.

The path segment from IV to V is determined in several steps. First, LST_1 from IV to V produces the potential curve (dashed line) in Figure 1, which shows a maximum at $P = 0.340$. Orthogonal optimization of $P = 0.340$ lowers its energy, as shown in Figure 1. LST_2 between the optimized structure for $P = 0.340$ and IV yields the dotted curve in Figure 1 having a maximum at $P = 0.462$. Orthogonal optimization of $P = 0.462$ between the optimized structure for $P = 0.340$ and IV lowers its energy to $P = 0.462$ on the lowest curve. The lowest potential curve in Figure 1 is a composite of LST_3, LST_4, and LST_5: LST_3 goes from V to the optimized structure for $P = 0.340$, LST_4 goes on to the optimized structure for $P = 0.462$, and LST_5 goes from there to IV. This potential curve shows a maximum near $P = 0.497$, which is not significantly lowered by further optimization, and we identify the structure corresponding to this point with the transition state for path 1. The final segment of path 1, from IV to III, is just given by LST_6 between these structures, and the potential curve this produces is shown as the last part of the lower curve in Figure 1. The entire path 1 potential curve is reproduced as line (a) in Figure 2.

Path 2 is given by a single segment between structures III and V, and it is determined in the same fashion as the segment between IV and V for path 1. Using the same path coordinates for the limiting structures III and V as we used for path 1, the calculation requires two orthogonal optimizations, the first at $P = 0.405$ and the second at $P = 0.608$. The final composite LST curve is shown as curve (b) in Figure 2. It shows a relative minimum at $P = 0.608$ and a relative maximum at $P = 0.55$. The relative maximum is not significantly affected by further optimization, and we identify it with the transition state on path 2.

The potential curves for paths 1 and 2 shown in Figure 2 are rather similar. First, each curve shows a decrease in energy from III to V interrupted by a relative minimum and a relative maximum. The minima are undoubtedly created by long-range attractive forces between the olefin π cloud and the vacant orbital of the boron atom; the maxima are created by short-range repulsive forces. Second, the numerical values of the energy at the maxima and minima for each path are almost the same. Since the reaction seems to be driven by the same influences along each path, we need to determine the extent to which the geometric and electronic structures of the two transition states are equivalent.

The similarity of the geometric structures is at once apparent. Table III compares some of the major parameters defining the two systems. The only sizable differences are the lengths of the C_2H_4 and B_3H_4 bonds. The atom H_4 is fixed by rather weak bonds in any model of the transition state considered here, so the rather small differences in Table III are not really significant. We see that the reaction passes through a loosely bound complex and subsequently through a transition state, but whether this is a simple concerted process such as in path 1 or involves a donation–back-donation intermediate as

Table IV. Potential Curve for the Formation of Ethylborane V and VI from a Complex of Borane and Ethylene (III) as a Function of Path Coordinate at the 4-31G Level

structure	III		IV				V	VI
P	1.0	0.667	0.585	0.497	0.462	0.340	0.0	
E^a	−104.272 51	−104.263 46	−104.257 36	−104.246 52	−104.245 99	−104.285 80	−104.315 96	−104.320 41
ΔE^b	−0.003 48	0.005 57	0.011 67	0.022 51	0.023 04	−0.016 77	−0.046 93	−0.051 38

[a] Energy in au. [b] Defined with respect to the sum of the 4-31G energies of borane (I) and ethylene (II) of −26.348 72 and −77.920 31 au, respectively.

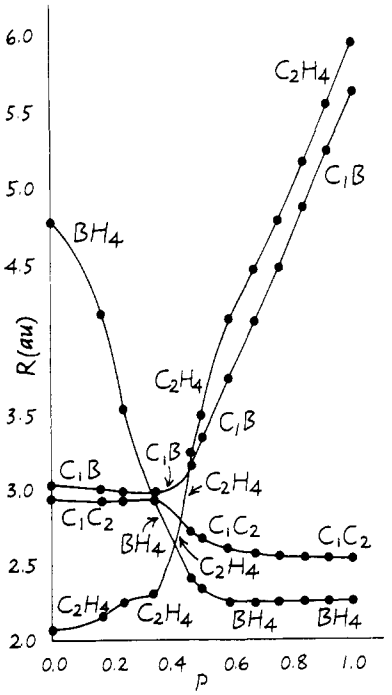

Figure 3. Variation of several geometry parameters with path coordinate for the reaction of a borane ethylene complex (III) to form ethylborane (V) via the intermediate IV.

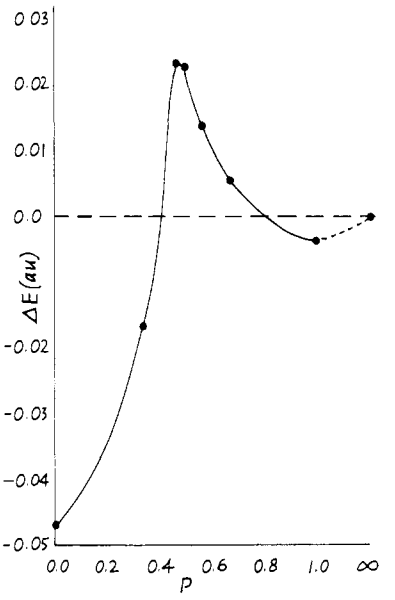

Figure 4. 4-31G potential curve for the reaction of a borane ethylene complex (III) to form ethylborane (V) via the intermediate IV.

in the dual mechanism called path 3 must be settled using more elaborate wave functions. In either case, the reaction does pass through the intermediate IV and over a transition state. All of these structures are defined by the molecular transformations referred to as path 1; their variations with path coordinate are shown in Table I and in Figure 3. All of the intermediate structures on paths 1 and 2 are constrained to have C_s symmetry.

Extended Basis Potential Curve

The PRDDO structures along path 1 are used to make an extended Gaussian basis set (4-31G) calculation of the potential curve. The calculation includes the structures I, II, III, IV, V, and VI and the interpolated points P = 0.340, 0.462, 0.497, and 0.669 from the LSTs performed in the determination of path 1. The resulting energies are shown in Table IV, and the potential curve is shown in Figure 4.

The quantitative particulars of the 4-31G curve are different from those of the PRDDO curve. It yields a reaction energy of −33 kcal/mol and an activation energy of 15 kcal/mol; both results are more in line with experiment,[2,32] but the addition of a correlation correction might well make the agreement better. In particular, the activation barrier might be lowered to near the experimental 2 kcal/mol.[32]

The 4-31G curve does have some qualitative similarities to the PRDDO results. First, both curves display a long-range minimum of energy created by the association of the olefin π bond and the vacant orbital on the boron atom. The precise location of this minimum is not clear in the 4-31G results, but in any case the minimum is very flat and the intermediate is only loosely bound. Second, both curves show a short-range maximum defining the transition state. Both curves place this maximum at nearly the same value of the path coordinate, which tends to make the PRDDO transition state structure credible.

Transition State Electronic Structure

Mulliken population analyses of the 4-31G wave functions were performed to assess the variations of the atomic charges and of certain overlap populations as functions of the path coordinate. The atomic charges are graphed in Figure 5.

The figure reveals several important features of the reaction. The first is the large donation of electron density to the boron atom near the transition state. The second is that this donation comes not from the unsaturated carbons of the olefin, which actually increase in electron density as the transition state forms from I and II, but rather from all of the hydrogen atoms attached to the structure. A substantial donation is made by the olefinic hydrogens H_5, H_6, H_7, and H_8, and a substantial donation is made by the borane hydrogens H_9 and H_{10}, but the largest single donation comes from the borane hydrogen H_4. The third feature of the reaction is that the two olefin carbon atoms acquire a substantial charge separation. As the transition state forms from I and II, C_1, which is closest to B_3, acquires a more negative charge than does C_2, which is close to the borane hydrogen H_4. After the system passes over the transition state toward the organoborane, a large charge transfer is made from the atoms B_3 and H_4 to the rest of the molecule. Some of this electron density ends up on atoms C_1 and C_2, although more of it goes to C_2 and tends to reduce the charge separation between these atoms.

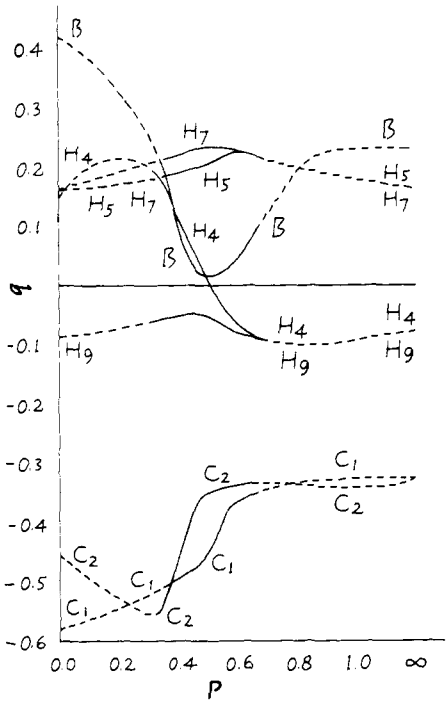

Figure 5. Variation of the atomic charges for the 4-31G wave functions with path coordinate for the reaction of a borane ethylene complex (III) to form ethylborane (V) via the intermediate IV.

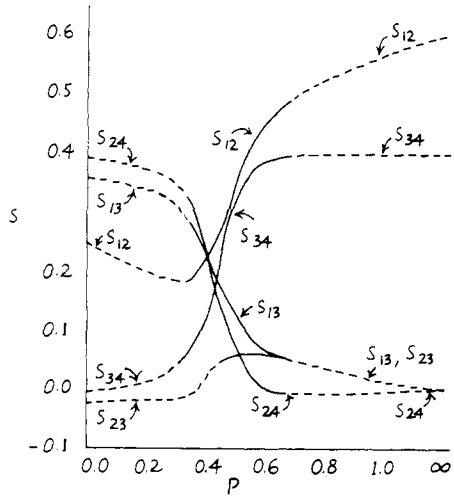

Figure 6. Variation of selected overlap populations for the 4-31G wave functions with path coordinate for the reaction of a borane ethylene complex (III) to form ethylborane (V) via the intermediate IV.

As the transition state forms from I and II, Figure 5 shows that more electron density is lost from atoms H_4, H_7, and H_8 than from atoms H_9, H_{10}, H_5, and H_6. This charge is transferred to both atoms B_3 and C_1, so one concludes that the major direction of the electron transfer is along the C_2C_1 and H_4B_3 bonds in III rather than just from the olefin to the borane. Basically, the B_3 and C_1 atoms are populated at the expense of the rest of the molecule, and with reference to the illustration of IV we would say that the motion is from right to left. This direction of charge transfer accounts for the anti-Markownikoff addition to alkyl-substituted ethylenes, in the sense that a CH_3 donates more electrons than the H that it replaces. Thus, the transition state which is stabilized is that for which B adds to CH_2 rather than to CHR.

The charge distribution changes considerably on going from one side of the transition state to the other. The charge separation between C_1 and C_2 disappears as the reaction goes through the transition state from III to V. It is possible that this charge separation controls the directive effects of electron-donating and electron-withdrawing groups. Since the boron atom tends to bond to the more negative carbon atom in the transition state, any substituent that creates a substantial charge separation between C_1 and C_2 prior to the formation of the transition state will control the direction of addition.

The overlap populations as functions of the path coordinate are shown in Figure 6. The bonding in III and V, corresponding to the path coordinate $P = 1.0$ and 0.0, is unambiguous. In the transition-state region, however, there are several positive bonding directions between the important atoms C_1, C_2, B_3, and H_4. The relative magnitudes of the overlap populations between C_1 and C_2 and between C_1 and B_3 in this region suggest a σ bond and a weakened π bond between C_1 and C_2 and a weak bond between C_1 and B_3. Similarly, the overlap populations between B_3 and H_4 and between C_2 and H_4 suggest a weakened bond between B_3 and H_4 and the incipient formation of a bond between C_2 and H_4. In this picture, the transition state more closely resembles I and II than it does the organoborane V. This is to be expected, since the transition state is energetically much closer to I and II than to V. The existence of the bonding interactions between atoms C_1 and B_3 and between atoms C_2 and H_4 is unmistakable, though, and one must admit them as real features of the transition-state structure.

In summary, the transition state is a highly polarized structure, and the dynamics of its formation from I and II and its distortion into the organoborane V suggest that the process can legitimately be called a donation-back-donation mechanism. As the transition state is formed a donation is made to the boron atom, and as the reaction is completed these electrons are donated back to the rest of the molecule. The direction of the charge transfer as well as the original donors and final acceptors are not in complete accord with conventional thought on the matter, but the basic donation-back-donation process seems clearly evident in the population analysis. In the following, we will show how this mechanism accounts for an unusual correlation diagram.

Orbital Energies and Orbital Control

The reaction path considered here preserves one plane of symmetry, namely, the plane defined by the eclipsed ethylborane molecule. Using this symmetry element, each MO can be classified as A or A′ according to its transformation properties under the point group C_s. In the closed-shell molecules, there are nine occupied A orbitals including all three inner shells and three occupied A′ orbitals. The lowest unoccupied molecular orbital (LUMO) has A symmetry. This single symmetry element, however, does not allow the reactions to be classified using the Woodward-Hoffmann rules,[33] so an analysis of the orbital control of the reaction must be based directly on the correlation diagram, shown in Figure 7. The diagram is remarkable because so many orbitals show large changes in energy, even—or perhaps especially—the inner shells.

The variation of the LUMO energy is rather conventional. There are two maxima, one near $P = 0.8$ corresponding to net bonding interactions generating the loose complex such as structure III, and one near $P = 0.3$ corresponding to the formation of the C_1B_3 and C_2H_4 bonds in V. Between these maxima is a shallow minimum near $P = 0.5$. One is tempted to say that the minimum is indicative of antibonding interactions among the occupied orbitals, but an examination of the rest of the correlation diagram reveals only one significant maximum of orbital energy, and it is in orbital 3A, which is a boron inner shell.

The highest occupied molecular orbital (HOMO) energy is more or less constant over the whole course of the reaction;

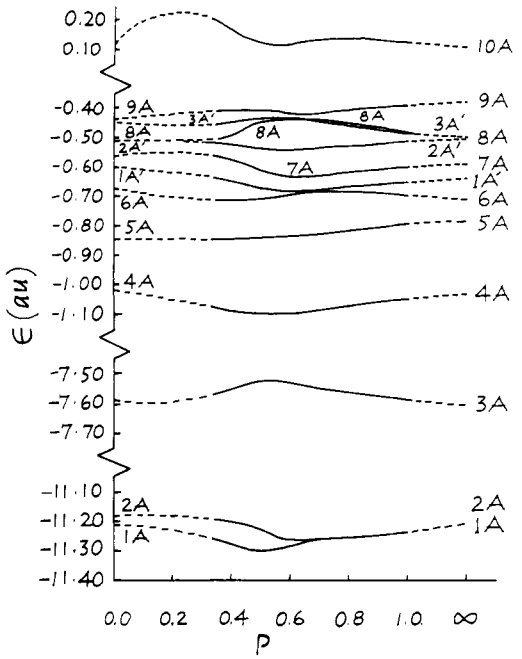

Figure 7. Orbital correlation diagram for the reaction of a borane ethylene complex (III) to form ethylborane (V) via the intermediate IV. Structure III corresponds to $P = 1.0$, while V corresponds to $P = 0.0$.

at least it seems so when compared to the behavior of some of the subjacent orbital energies. In some reactions, orbital control is maintained by the subjacent orbitals when they allow the formation of transition states that would normally be Woodward–Hoffmann forbidden,[34] but these situations normally involve the first one or two subjacent orbitals. In the hydroborations reaction, the orbital energies of even the lowest lying inner shells show large changes.

A close examination of the correlation diagram in conjunction with the population analysis discussed previously reveals it to be consistent with a polarized transition state structure, and it is consistent with our interpretation as proceeding via a donation–back-donation mechanism. The population analysis in Figure 5 shows a large donation to the boron atom from the hydrogen atoms, and one naturally expects this to be reflected in the orbital energies. Since the orbital energies of a negative ion are greater and the orbital energies of a positive ion are less than those of the neutral species, the MOs with contributions from the hydrogen atoms should decrease in energy as the transition state forms from I and II. There should also be a corresponding rise in the energy of the orbitals placing great weight on the boron atom. For I and II, $P = \infty$ in Figure 7, the orbitals 5A, 1A′, 7A, and 3A′ all contain large contributions from the olefin hydrogen atoms, and, as may be seen by tracing the energy curves from $P = \infty$ in toward the transition state, all but one of the orbitals, 3A′, decrease in energy. At $P = \infty$, the orbitals 6A, 2A′, and 8A all contain large contributions from the hydrogen atoms attached to the borane subunit. As these curves are traced from $P = \infty$ in toward the transition state, orbitals 6A and 2A′ decrease in energy, but orbital 8A increases in energy. At $P = \infty$ orbital 8A is a member of a degenerate pair of borane orbitals and it transforms as a p orbital directed at the hydrogen H_4, so this orbital has a large contribution from both B_3 and H_4. As the transition state forms from I and II, H_4 depopulates, but much of this population is shifted to B_3, and as a result orbital 8A has a fairly stable energy but does undergo a slight promotion. After the transition state is passed, Figure 5 shows that both B_3 and H_4 depopulate, so orbital 8A ought to decrease in energy. Indeed it does, as seen in Figure 7 between $P = 0.5$ and 0.4. Of course the boron atom is a major recipient of electron density during the transition-state formation, so some orbital associated with it must be sharply promoted, and, as seen in Figure 7, the boron inner shell 3A has a sharp maximum of energy near $P = 0.5$.

Table V. Orbital Exponents for the Slater Orbital Basis

atom	1s	2s	2s′	2p	2p′
B[a]	4.679	1.413	0.876	2.217	1.006
C[a]	5.673	1.831	1.153	2.730	1.257
H[b]	1.504	1.434			

[a] Reference 36. [b] Reference 37.

The fact that a large population shift is reflected in large changes in the energy of inner shells is not surprising. For instance, the inner-shell energies of the ground states of the boron atom and its (−1) ion are −7.695 and −7.425 au, respectively; the corresponding energies for carbon are −11.326 and −10.956 au.[35] Given that the transition-state formation is accompanied by a population shift of almost one-half electron on the boron atom, the observed change in its inner-shell energy is very understandable. The carbon atom charges shift by almost ¼ au, so we must anticipate large shifts in the carbon inner shells as well.

Indeed, the behavior of the carbon inner shells is especially interesting. As shown in Figure 7, they are degenerate in the separated systems I and II, and they remain nearly so until the transition state starts to form near $P = 0.6$. From $P = 0.6$ to $P = 0.5$ the orbital near degeneracy is broken with orbital 2A increasing and orbital 1A decreasing in energy. From the population analysis in Figure 5, it is apparent that the total charges on the two carbons are also diverging in this region, and that one of the carbons, C_1, is acquiring a much more negative charge than the other carbon C_2. That being the case, one would expect the MO dominated by C_1 to be higher in energy than the MO dominated by C_2, and an inspection of the MO expansion coefficients confirms this hypothesis. After the transition state is formed and the reaction passes on to form the organoborane, Figure 5 shows ($P \leq 0.45$) that both B_3 and H_4 depopulate and donate electron density to the olefin, so the boron inner shell should decrease in energy as should orbital 8A which is dominated by the hydrogen H_4. The carbon inner shells should show a concomitant increase in energy, as should all the orbitals having large contributions from the olefin hydrogen atoms. Examination of the correlation diagram bears out these conjectures.

In summary, the existence of a polarized donation–back-donation transition state is suggested by the population analysis, and it is confirmed by a close analysis of the orbital correlation diagram. The correlation diagram shows that many orbitals undergo large shifts in energy, and some of the largest shifts are observed in terms of simple concerted bond rearrangements, but it is seen to be a natural consequence of the donation–back-donation transition state such as discussed above.

Correlation Corrections

As we note, the effect of basis-set extension drastically affects the values of the reaction and activation energies, and the effects of the correlation energy must also be considered. To do so, zero-order configuration interaction (CI) calculations are performed on I, II, the transition state at $P = 0.462$, and VI. The excitations are made from the closed-shell wave functions for each system and include all the single and double excitations from the valence orbitals to the virtual orbitals that would be defined by a minimal basis set calculation.

The SCF calculations use MOs expanded in an extended

Table VI. Slater Orbital and Zero-Order CI Calculations of the Reaction and Activation Energy[a] of the Hydroboration Reaction

system	I	II	$P = 0.462$	VI
SCF	−26.353 22	−77.948 96	−104.281 91	−104.364 59
CI	−26.369 47	−78.033 51	−104.418 88	−104.474 18
Δ(SCF)[b]			−0.020 27	−0.062 42
Δ(CI)[b]			−0.015 90	−0.071 20

[a] Energy in au. [b] $\Delta = E - E_I - E_{II}$.

basis of Slater orbitals. The valence orbitals for all the atoms are described by a double ζ basis, and the inner shells on boron and carbon are described by a single function. The boron and carbon exponents are from Clementi and Roetti,[36] and the hydrogen exponents are from McDowell;[37] they are shown in Table V. SCF calculations produce the Hartree–Fock energies reported in Table VI.

The CI calculations yield the total energies and reaction energies shown in Table VI. The reaction energy for the formation of VI from I and II is −45 kcal/mol. This is exothermic with respect to experiment,[23] but, considering the limited CI performed here, it is not an unreasonable prediction. The reaction energy for the formation of IV from I and II is −10 kcal/mol, so at the zero-order CI level the reaction goes without activation.

Clearly the correlation effect stabilizes the transition state relative to I and II and to VI. The transition state is known to have two weakened bonds and two partially formed bonds, and a preliminary analysis of the PRDDO localized orbitals suggests that the transition state is actually dominated by two three-center bonds, one over $C_1C_2B_3$ and one over $B_3H_4C_2$. If that interpretation can be made of the extended basis wave function, then the correlation energy stabilization of the transition state is to be expected, since the correlation energy in three-center bonds is generally larger than in two-center bonds.

Comparison to Other Studies

While this manuscript was in preparation, two other detailed studies of the hydroboration reaction have appeared. In a MNDO study, Dewar and McKee[38] have calculated a similar minimum energy reaction pathway for the addition of borane to ethylene, but find an overall barrier of 7.6 kcal/mol for the forward reaction. Clark and Schleyer[39] concur with our findings of a zero activation energy for hydroboration based on calculations at the STO-3G and 4-31G levels. However, they did not include the effects of configuration interaction.

Acknowledgment. One of the authors (K.R.S.) is grateful to the National Science Foundation for an Energy Related Postdoctoral Fellowship for the academic year 1977–1978. Another author (G.D.G.) thanks the National Science Foundation for a Predoctoral Fellowship. We wish to thank the National Science Foundation for support (Grant CHE77-19899), and we also thank Ms. Jean Evans for preparing the illustrations.

References and Notes

(1) 229 RB #1 PRC, Phillips Petroleum Co., Bartlesville, Okla. 74004.
(2) H. C. Brown, "Hydroboration", W. A. Benjamin, New York, 1962.
(3) G. M. L. Cragg, "Organoboranes in Organic Synthesis", Marcel Dekker, New York, 1973.
(4) H. C. Brown, "Organic Synthesis via Boranes", Wiley, New York, 1975.
(5) H. C. Brown and B. C. Subba Rao, *J. Am. Chem. Soc.*, **81**, 6423 (1959).
(6) H. C. Brown and G. Zweifel, *J. Am. Chem. Soc.*, **82**, 4708 (1960).
(7) H. C. Brown and G. Zweifel, *J. Am. Chem. Soc.*, **83**, 2544 (1961).
(8) G. Zweifel, N. R. Ayyangar, and H. C. Brown, *J. Am. Chem. Soc.*, **85**, 2072 (1963).
(9) E. F. Knights and H. C. Brown, *J. Am. Chem. Soc.*, **90**, 5281 (1968).
(10) S. P. Acharya, H. C. Brown, A. Suzuki, S. Nozawa, and M. Itoh, *J. Org. Chem.*, **34**, 3015 (1969).
(11) H. C. Brown and R. L. Sharp, *J. Am. Chem. Soc.*, **88**, 5851 (1966).
(12) J. Klein, E. Dunkelblum, and M. A. Wolff, *J. Organomet. Chem.*, **7**, 377 (1967).
(13) D. J. Pasto and S. Z. Kang, *J. Am. Chem. Soc.*, **90**, 3797 (1968).
(14) B. R. Ree and J. C. Martin, *J. Am. Chem. Soc.*, **92**, 1660 (1970).
(15) A. Streitwieser, L. Verbit, and R. Bittman, *J. Org. Chem.*, **32**, 1530 (1967).
(16) D. J. Pasto and F. M. Klein, *J. Org. Chem.*, **33**, 1468 (1968).
(17) P. R. Jones, *J. Org. Chem.*, **37**, 1886 (1972).
(18) T. A. Halgren and W. N. Lipscomb, *Proc. Natl. Acad. Sci. U.S.A.*, **69**, 652 (1972).
(19) T. A. Halgren and W. N. Lipscomb, *J. Chem. Phys.*, **58**, 1569 (1973).
(20) T. A. Halgren and W. N. Lipscomb, *Chem. Phys. Lett.*, **49**, 225 (1977).
(21) T. A. Halgren, to be published.
(22) R. Ditchfield, W. J. Hehre, and J. A. Pople, *J. Chem. Phys.*, **54**, 724 (1971).
(23) D. J. Pasto, B. Lepeska, and T.-C. Cheng, *J. Am. Chem. Soc.*, **94**, 6083 (1972).
(24) R. F. Stewart, *J. Chem. Phys.*, **50**, 2485 (1969).
(25) W. J. Hehre, R. F. Stewart, and J. A. Pople, *J. Chem. Phys.*, **51**, 2657 (1969).
(26) J. A. Pople, *Acc. Chem. Res.*, **3**, 217 (1970).
(27) Gaussian calculations were performed using the program GAUSSIAN 70: W. J. Hehre, W. A. Lathan, M. D. Newton, R. Ditchfield, and J. A. Pople, Program No. 236, Quantum Chemistry Program Exchange, University of Indiana, Bloomington, Ind.
(28) B. P. Stoicheff, *Can. J. Phys.*, **33**, 811 (1955).
(29) W. E. Palke and W. N. Lipscomb, *J. Chem. Phys.*, **45**, 3948 (1966).
(30) J. A. Pople and M. S. Gordon, *J. Am. Chem. Soc.*, **89**, 4253 (1967).
(31) J. D. Dill, P. v. R. Schleyer, and J. A. Pople, *J. Am. Chem. Soc.*, **98**, 1663 (1976).
(32) T. P. Fehlner, *J. Am. Chem. Soc.*, **93**, 6366 (1971).
(33) R. B. Woodward and R. Hoffmann, "The Conservation of Orbital Symmetry", Verlag Chemie, Weinheim/Bergstr., Germany, 1966.
(34) J. A. Berson, *Acc. Chem. Res.*, **5**, 406 (1972).
(35) E. Clementi, "Tables of Atomic Functions", a supplement to a paper by Enrico Clementi, *IBM J. Res. Dev.*, **9**, 2 (1965).
(36) E. Clementi and C. Roetti, *At. Data Nucl. Data Tables*, **14**, 3–4 (1974).
(37) H. K. McDowell, Ph.D. Thesis, Harvard University, 1972.
(38) M. J. S. Dewar and M. L. McKee, *Inorg. Chem.*, **17**, 1075 (1978).
(39) T. Clark and P. v. R. Schleyer, *J. Organomet. Chem.*, **156**, 191 (1978).